Journal of Applied Polymer Science

Porous and Spherical Hydroxyapatite Microcomposites for Immunoglobulin G Adsorption

Birnur Akkaya
Department of Molecular Biology and Genetics, Faculty of Science, Cumhuriyet University, Sivas 58140, Turkey
Correspondence to: B. Akkaya (E-mail: pergamonchem@gmail.com)

ABSTRACT: A novel porous and spherical hydroxyapatite (HA) microcomposite with an average diameter of 50–100 μm was produced by suspension polymerization for the adsorption of human immunoglobulin G (IgG). The specific surface area of the pure HA and HA microcomposite were found to be 80.25 and 182.53 m^2/g, respectively. Characterizations were performed with X-ray diffraction, Fourier transform infrared spectroscopy, thermogravimetric analysis, and scanning electron microscopy analysis. The swelling ratio of the spherical HA microcomposites was 170%. The maximum adsorption of IgG from aqueous solution was observed at pH 7.0 (5 m*M* phosphate buffer) and at 45°C in a batch system in which parallel separate experiments were performed independently. An IgG adsorption capacity value of up to 140 mg/g was obtained for the HA microcomposite. The IgG molecules could be repeatedly adsorbed and desorbed through the use of spherical microcomposites without a noticeable loss in the IgG adsorption capacity. © 2013 Wiley Periodicals, Inc. J. Appl. Polym. Sci. 000: 000–000, 2013

KEYWORDS: adsorption; biomaterials; biomedical applications; proteins

Received 23 January 2013; accepted 26 March 2013; Published online 00 Month 2013
DOI: 10.1002/app.39341

INTRODUCTION

Immunoglobulin G (IgG) adsorption onto solid surfaces is very important for biomedical applications, such as immunoassays and biosensors. Antibodies, which are biologically active glycoproteins, are produced by plasma cells in response to the presence of foreign substances. They offer exciting potential as diagnostic and therapeutic reagents and could be used as affinity ligands to purify other pharmaceutically important proteins, such as cytokines and blood-clotting factors.[1,2] In the development of diagnostic reagents, the stable attachment, including the selectivity and specificity, of IgG molecules to solid surfaces without the disruption or masking of biological functions is the main goal to be achieved for proteins.[3] The downstream processing of antibodies could constitute most of the manufacturing costs. To develop a downstream process, efficient and well-designed product recovery methods are very essential. In addition, IgG removal from human plasma is used for the treatment of immune disorders, such as systemic lupus erythematosus, alloimmunization, and cancer.[4,5] There have been some investigations with hydroxyapatite (HA)[6,7] and different affinity adsorbents for antibody adsorption.[8–10]

HA is a cost-effective chromatographic material, which also have some advantages, including a high stability,[11–13] high adsorption capacity, high selectivity,[14] resistance to biochemical degradation, and low toxicity.[15] HA is a biocompatible and bioactive material,[16] which has been used in a wide range of applications, such as the separation of biomolecules (IgG)[17–19] and clinical applications,[20–22] including drug-delivery systems and bone tissue engineering. In addition its advantages, the composite (HA/polymer) can behave more effectively than pure HA as an adsorbent (the aggregation and coagulation of HA limits its adsorptive features). These composite structures resemble a guest and host because HA is dispersed in the polymer structure. The swelling properties of the inert polymer part provide easy diffusion.[23] So when the surface area and diffusion are increased, the available adsorptive sites are increased. The shape of HA also varies according to its application area, for example, in rods, needles, plates, or microspheres.[24] Recently, ethylene vinyl acetate (EVA) has been used as a binder, such as to obtain spherical composites and HA particles of spherical shape.[25] Spherical HA microcomposites have been shown to be more biocompatible,[26,27] and, furthermore, it has been claimed that irregular particles could produce inflammatory effects.[28]

Various methods have been reported for the synthesis of spherical HA microcomposites.[29–31] In this study, suspension polymerization was used to synthesize porous and spherical HA microcomposites.

The aim of this study was to prepare a novel porous and spherical HA microcomposite affinity adsorbent for the adsorption of human immunoglobulin G (h-IgG) from

© 2013 Wiley Periodicals, Inc.

aqueous solution. The study was performed in three main steps: (1) the synthesis of HA, with a chemical reaction between $Ca(OH)_2$ and H_3PO_4; (2) the preparation of the porous and spherical HA microcomposites including HA 50–100 μm in diameter by suspension polymerization in the presence of ethylene glycol dimethacrylate (EGDMA), poly(vinyl alcohol), and benzoyl peroxide; and (3) adsorption of the h-IgG on pure HA and porous and spherical HA microcomposite material in aqueous media with different amounts of h-IgG and ionic strengths at differing pH points and temperatures. The HA microcomposite was characterized by scanning electron microscopy (SEM), Fourier transform infrared (FTIR) spectroscopy, X-ray diffraction (XRD), thermogravimetric analysis (TGA), Brunauer–Emmett–Teller (BET) characterization, and swelling tests. The desorption of h-IgG and the reusability of the HA microcomposites were also tested.

EXPERIMENTAL

Chemicals

h-IgG (lyophilized) was supplied by Sigma (St Louis, MO). EGDMA was obtained from Fluka AG (Buchs, Switzerland). Benzoyl peroxide was obtained from Fluka. Poly(vinyl alcohol) (molecular weight = 85.000–140.000 Da, 98% hydrolyzed) was supplied from Sigma-Aldrich (Steinheim, Germany). The buffer solutions were prefiltered through a 0.2-μm membrane (Whatman, Dassel, Germany). All glassware was extensively washed with dilute nitric acid before use. All other chemicals were of analytical-grade purity and were purchased from Merck AG (Darmstadt, Germany).

Synthesis of HA and Spherical HA Microcomposites

The synthesis of the starting material, HA, was obtained by a chemical reaction between $Ca(OH)_2$ and H_3PO_4 and sintered at high temperature.[32]

The spherical HA microcomposites were prepared under suspension polymerization. The following experimental procedure was applied for the synthesis of the spherical HA microcomposites. An amount of 200 mg of poly(vinyl alcohol) (the stabilizer) was dissolved in 50 mL of deionized water for the preparation of the continuous phase. For the preparation of dispersion phase, 8.0 mL of EGDMA (the crosslinker), 1.0 g of HA powder, and 12.0 mL of toluene (a pore maker) were mixed in a beaker. An amount of 100 mg of benzoyl peroxide (the initiator) was dissolved in this homogeneous solution. The dispersion phase was added to the continuous medium in a glass-sealed polymerization reactor (100 mL) placed in a water bath equipped with a temperature-control system. The polymerization reactor was heated to 65°C with stirring of the polymerization medium at 500 rpm for 2 h. During the reaction after polymerization, the reactor content was cooled at room temperature. To remove the diluent and any possible unreacted monomers and other ingredients from the beads, a washing procedure was applied after polymerization. The suspension was stirred for about 1 h at room temperature, and the beads were separated by filtration. When not in use, to prevent microbial contamination, the beads were kept under refrigeration in a 0.02% sodium azide solution.[33]

Characterization of the HA Microcomposites

The surface area and pore diameters of the pure HA and porous and spherical HA microcomposites were determined by the BET equation with a nitrogen adsorption system at 77 K and a Quantachromosorb Instrument. Screen analysis performed with standard test sieves (Retsch GmbH and Co., Germany) was used to determine the average size and size distribution of the porous and spherical HA microcomposite. The mean particle size was obtained by measurement of the diameter of 200 particles in each SEM micrograph for pure HA. Water-uptake studies of the HA microcomposites were performed in distilled water. The water content of the spherical HA microcomposites was calculated with the weights of the microcomposite before and after the uptake of water. The surface morphology was examined with an SEM instrument (model JSM 5600, JEOL, Japan).

For the characterization of the chemical structure of the microcomposites, FTIR spectra were obtained with an FTIR spectrophotometer (Mattson 1000, United Kingdom). For the powder diffraction of the microcomposites, XRD was performed with a Rigaku Dmax 2200 (2θ/min scan rate) with Cu Kα radiation ($\lambda = 1.5418$ Å). Dried particles were mounted on a sample holder, and the patterns were recorded in the range 10–50 at a speed of 5 m/min to determine the crystallinity. TGA was performed by a PerkinElmer instrument (Diamond).

Adsorption of h-IgG from Aqueous Solutions

The adsorption of h-IgG on the pure and spherical HA was studied in a batch system. The microcomposites were incubated with 5 mL of h-IgG solution for 2 h in the reservoir by magnetic stirring with 0.03 g of HA and the microspheres individually. To determine the effect of the initial concentration of h-IgG on the adsorption, the amount of h-IgG was varied between 0.5 and 5.0 mg/mL. The h-IgG adsorption from aqueous solution was investigated at different pH values; these solutions included acetate buffer (5 m*M*, pH 5.0), phosphate buffer (5 m*M*, pH 6.0–8.0), and carbonate buffer (5 m*M*, pHs 9 and 10). The following temperatures were used to study the temperature effects on adsorption: 4, 15, 25, 35, and 45°C. To investigate the effect of the ionic strength on the adsorption, the amount of NaCl was changed in the range 0.01–1.0*M*. The h-IgG concentration was estimated from its absorbance at 280 nm in a ultraviolet–visible spectrophotometer (Optima, Tokyo) with a molar absorptivity of 13.6 for a 1% solution of h-IgG. The amount of the adsorbed h-IgG/dry microcomposite (Q) was calculated with the concentrations of h-IgG in the initial solution and at equilibrium with the following equation:

$$Q = (C_i - C_f)V/m \quad (1)$$

where C_i and C_f are the initial and final IgG concentrations (mg/mL), respectively; V is the volume of the protein solution (mL); and m is the amount of bead used (g).

Desorption and Repeated Use

The desorption of h-IgG from the microcomposites was performed in a buffered solution containing 1.0*M* NaCl at pH 7.0. The h-IgG adsorbed microcomposites were placed in the desorption medium and stirred for 1 h at room temperature at a stirring rate of 150 rpm. The final h-IgG concentration within

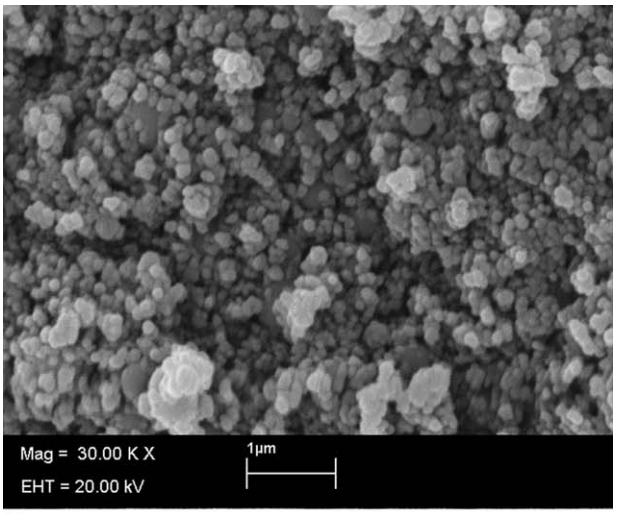

(a) SEM images of pure hydroxyapatite

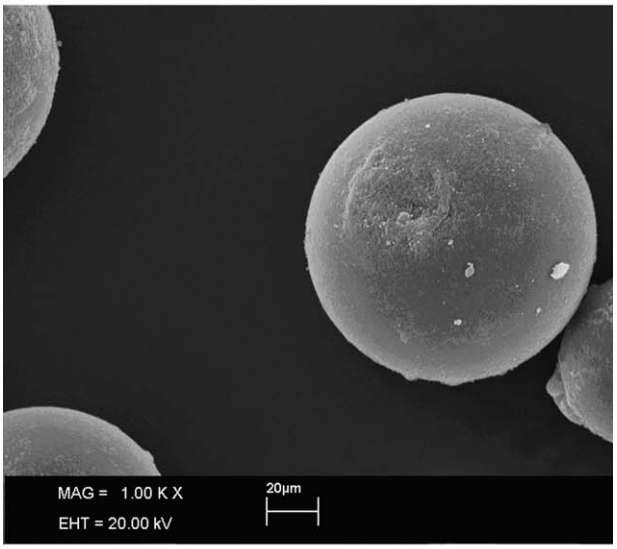

(b) SEM photographs of porous and spherical hydroxyapatite microcomposite

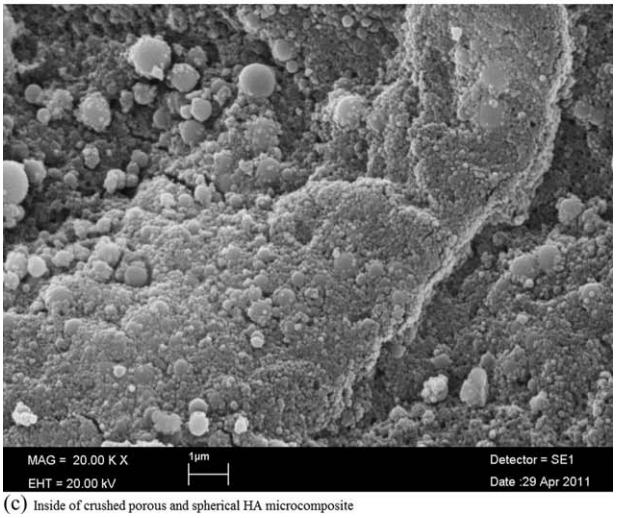

(c) Inside of crushed porous and spherical HA microcomposite

Figure 1. (a) SEM image of the pure HA. (b) SEM photograph of the porous and spherical HA microcomposite. (c) Inside of the crushed porous and spherical HA microcomposite. [Color figure can be viewed in the online issue, which is available at wileyonlinelibrary.com.]

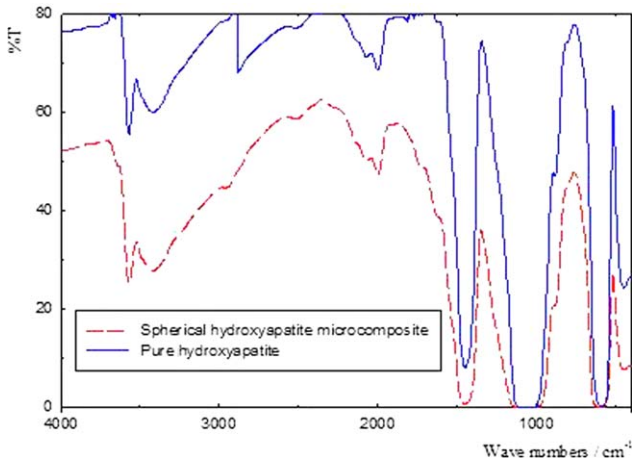

Figure 2. FTIR spectra of the pure HA (straight line) and spherical HA microcomposites (dotted line). [Color figure can be viewed in the online issue, which is available at wileyonlinelibrary.com.]

the desorption medium was determined by spectrophotometry. The desorption ratio was calculated from the amount of h-IgG adsorbed on the microcomposites and the amount of h-IgG desorbed. h-IgG adsorption–desorption cycles were performed five times with the same microcomposites to test their reusability.

RESULTS AND DISCUSSION

Properties of the HA and Spherical HA Microcomposites

The porous and spherical HA microcomposites were obtained by EGDMA (organic material) and HA (inorganic material). The equilibrium water-uptake ratio of the spherical HA was 170%, whereas the equilibrium water-uptake ratio of the pure HA was 60%. As shown in the results, the water-uptake ratio of the spherical HA microcomposites increased. This was because of the dispersed hydrophilic groups in the produced polymeric microcomposite, which could attract more water molecules to the polymer matrices. In addition, HA in the composite decreased the degree of crosslinking and increased the water-uptake behavior.

The radical suspension polymerization procedure provided spherical HA in the diameter range of 50–100 μm (diameter of pure HA $<$ 250 nm). The BET surface areas of the pure HA and spherical HA were 72.25 and 182.53 m^2/g; the surface area was increased by obtaining microcomposites. This provided the adsorbent with high protein adsorption features. On the basis of these results, we concluded that the porous and spherical HA microcomposite had effective pore structures (the pore diameter of pure HA was 6 nm, and that of the porous and spherical HA microcomposite was 50 nm) for the liquid chromatographic separation of h-IgG compared with the nonporous and nonspherical pure HA.

The surface morphology of the pure HA and porous and spherical HA microcomposite were recorded by SEM analysis. As is clearly shown in Figure 1, the porous and spherical HA microcomposite had a spherical form [Figure 1(b)] because of the pores that were formed during the polymerization procedure. The presence of pores within the spherical microcomposite is

Applied Polymer SCIENCE

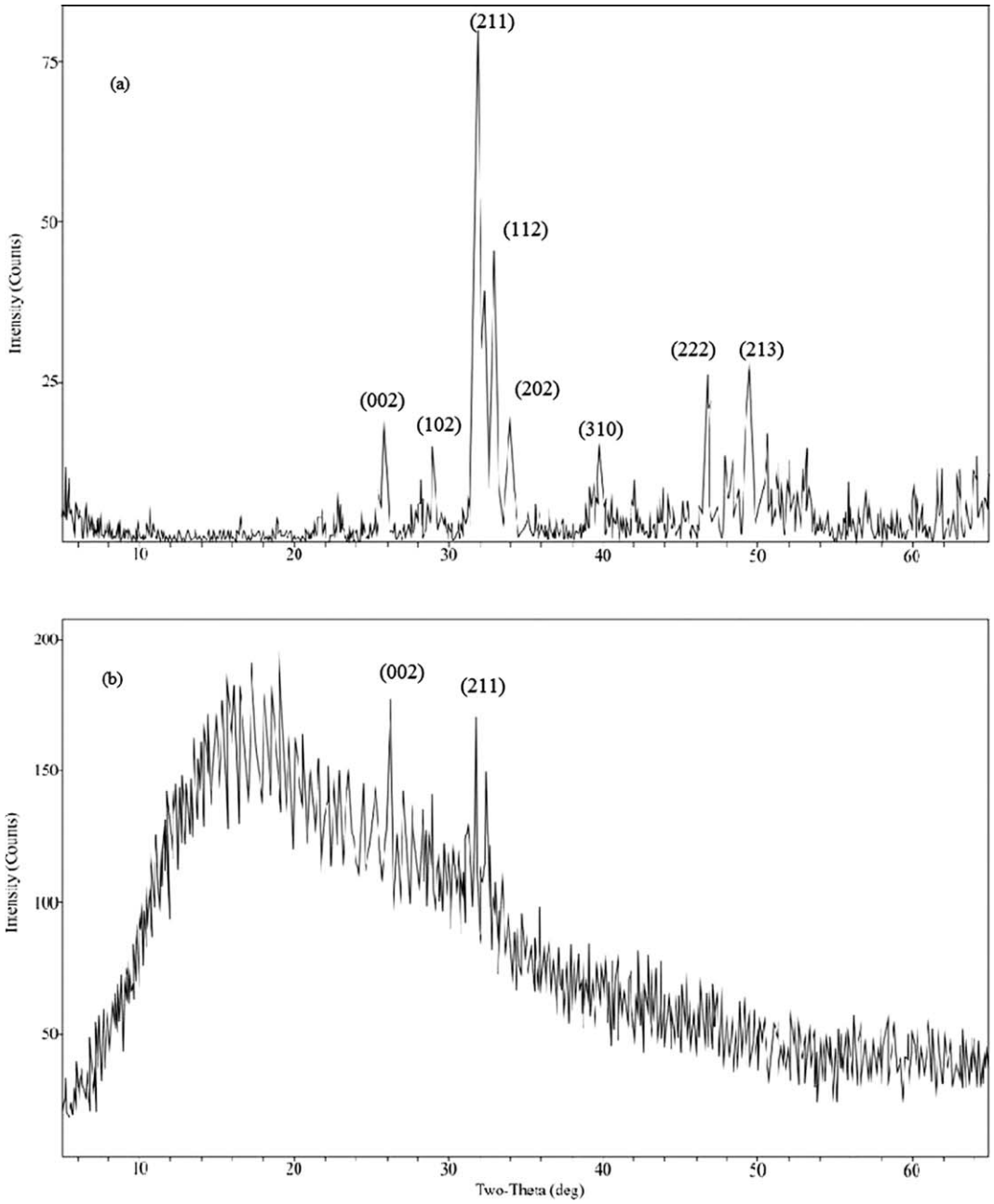

Figure 3. XRD patterns of the (a) pure HA and (b) porous and spherical HA microcomposite.

clearly shown in the micrograph [Figure 1(a)]. We concluded that spherical HA had a porous core in the dry state [Figure 1(c)].

The FTIR spectra both of the microcomposites are shown in Figure 2. As shown in Figure 2, the 450-, 6000-, 961-, and 1023-cm^{-1} peaks were typical frequencies of the PO_4 groups of HA. The peak at 3500 cm^{-1} showed —OH stretching.[34,35] The peaks between 1600 and 1750 cm^{-1} appeared because of the carbonyl stretches of EGDMA, which was incorporated into the structure. There were also C—H bending bands in the frequency range 1200–1400 cm^{-1}, and there was also a hydroxyl band at 3500 cm^{-1}. There was no a significant difference between the two FTIR spectra, and this showed that there was good incorporation of HA with EGDMA without any interaction or chemical bound in the porous and spherical HA microcomposites.[36] The porous and spherical HA microcomposites showed the main characteristic peaks of HA and EGDMA.

Figure 3 presents the XRD patterns of the microcomposites. As shown in Figure 3, all of the peaks were typical for HA ($2\theta = 26$, 32, and 34°). As compared with pure HA, peak broadening was due to the amorphous contribution of EGDMA ($2\theta = 16°$).[26,36] The typical HA peaks also existed in the XRD patterns of the porous and spherical microcomposite structure.

Figure 4 shows the thermogravimetric decomposition of the pure HA and porous spherical HA microcomposite at temperatures within the range 50–800°C. As shown in Figure 4, because

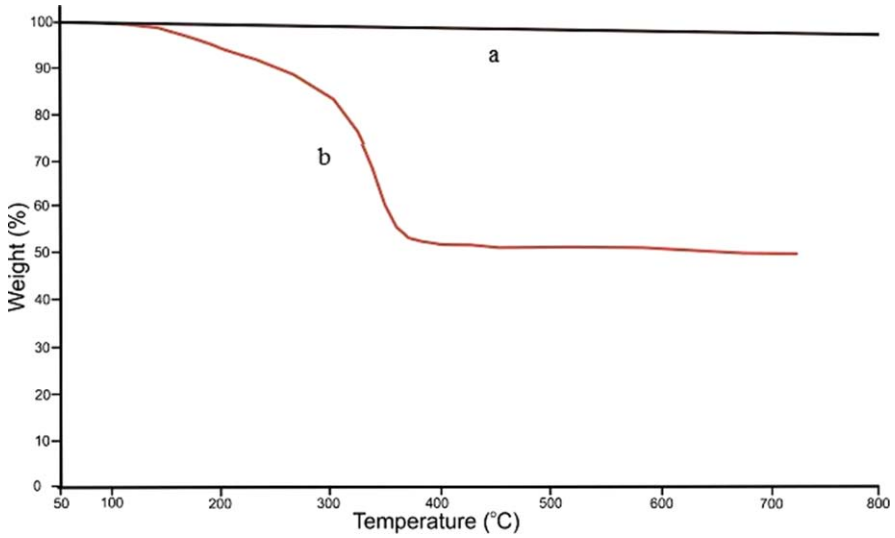

Figure 4. TGA curves of the (a) pure HA and (b) porous and spherical HA microcomposite. [Color figure can be viewed in the online issue, which is available at wileyonlinelibrary.com.]

of the high thermal stability of HA, there was an insignificant weight loss of about 1.25% up to 800°C. This was due to the evaporation of water. The decomposition of the porous and spherical HA microcomposite occurred in three steps: the weight loss of 8% at 100–200°C was due to solvent evaporation, that of 15% at 300°C was due to the partial degradation of EGDMA, and that of 50% at 400°C was due to the complete degradation of EGDMA, but there was no further degradation above 400°C. This indicated the existence of EGDMA in the structure. Thus, the incorporation of HA in the microcomposite could be calculated from the TGA. After the removal of the polymer, 50% of the total weight of the microcomposite remained.

Adsorption of h-IgG from Aqueous Solutions

Effect of the h-IgG Concentration. Figure 5 shows the effect of the initial h-IgG concentration on adsorption. As presented in the figure, when the h-IgG concentration was increased, the adsorbed amount of h-IgG increased. Because of the high driving force, the adsorption rate increased with increasing h-IgG concentration. At the beginning of the adsorption process, there was a relatively faster adsorption rate (because of the high h-IgG concentration at the beginning), and then, the adsorption equilibrium was achieved in about 120 min (at the end of adsorption, there was a low h-IgG concentration). The maximum adsorption capacity was 140 mg/g of microcomposite, whereas the pure HA had only a 20 mg/g adsorption capacity. This was because of the porosity, high surface area, and water uptake of the polymer part, which had a negligible adsorption capacity toward IgG.[37,38] Thus, increasing the available adsorptive sites (maybe surface functional groups) may have caused an increase in the adsorption behavior of the porous and spherical HA microcomposite. As shown in the results, the HA microcomposites could be used as an effective adsorbent for antibodies.[39]

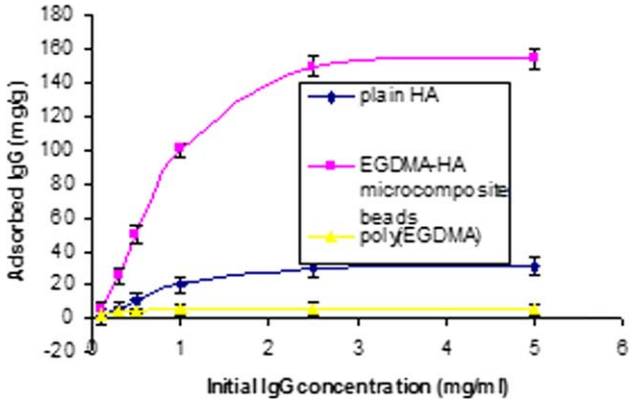

Figure 5. Effect of the initial concentration of h-IgG on the adsorption capacity [pH 7.0 (phosphate buffer), temperature = 25°C]. [Color figure can be viewed in the online issue, which is available at wileyonlinelibrary.com.]

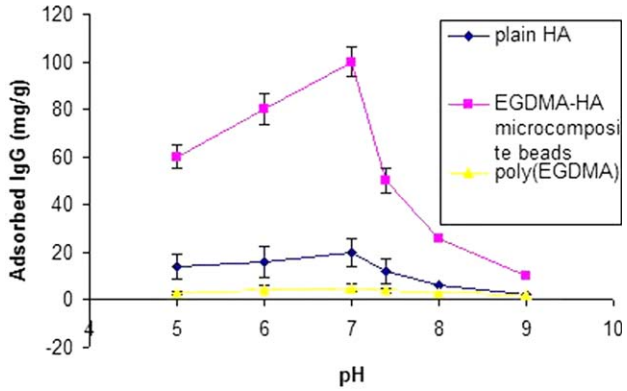

Figure 6. Effect of the pH on the h-IgG adsorption and h-IgG concentration (1.0 mg/mL, temperature = 25°C). [Color figure can be viewed in the online issue, which is available at wileyonlinelibrary.com.]

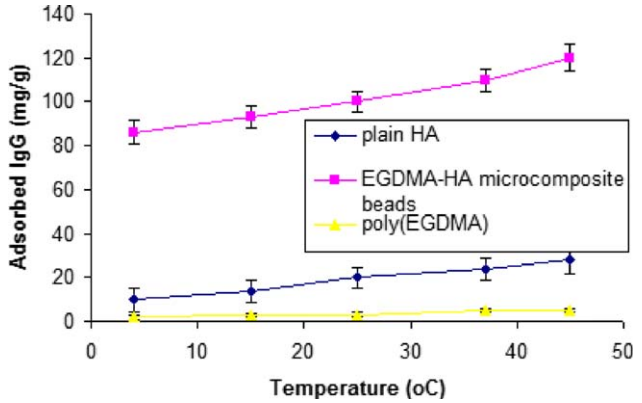

Figure 7. Effect of the temperature [pH 7.0 (phosphate buffer), h-IgG concentration = 1.0 mg/mL]. [Color figure can be viewed in the online issue, which is available at wileyonlinelibrary.com.]

Effect of pH. The adsorption of h-IgG on the pure HA and spherical HA microcomposites as a function of pH is given in Figure 6. The amount of adsorbed h-IgG showed a maximum at pH 7.0 (5 m*M* phosphate buffer), with a decrease at lower and higher pH values (the isoelectric point of h-IgG was 6.2). At a pH value of 7.0, electrostatic interactions were generated that were dependent on the surface charges between the negatively charged phosphate groups and positively charged amino groups.[35] At pH values lower and higher than pH 7.0, the adsorbed amount of h-IgG decreased because of the decreasing number of interactions {poly(ethylene glycol dimethacrylate) [poly(EGDMA)] had a negligible adsorption capacity toward IgG}.

Effect of the Temperature. Figure 7 shows the temperature effect of h-IgG adsorption on the pure HA and porous and spherical HA microcomposites. Up to 45°C, the adsorption was efficient, and there was a slight increase in the adsorption capacity by about 20% because of the increasing diffusion rate into the microcomposites [poly(EGDMA) had a negligible adsorption capacity toward IgG]. An **increase** in the **temperature** increased the **adsorption capacity** of the porous and spherical HA microcomposites because of the endothermic and

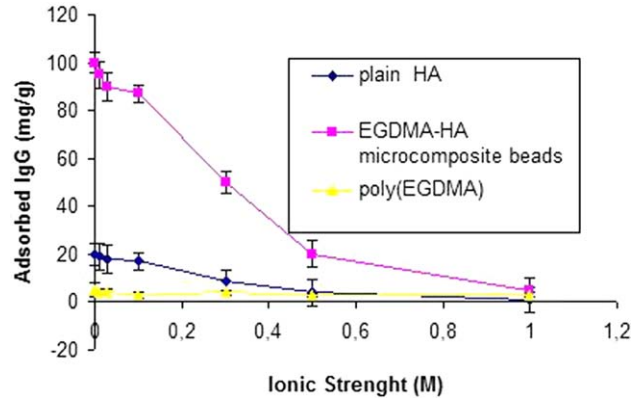

Figure 8. Effect of the ionic strength [pH 7.0 (phosphate buffer), temperature = 25°C, h-IgG concentration = 1.0 mg/mL]. [Color figure can be viewed in the online issue, which is available at wileyonlinelibrary.com.]

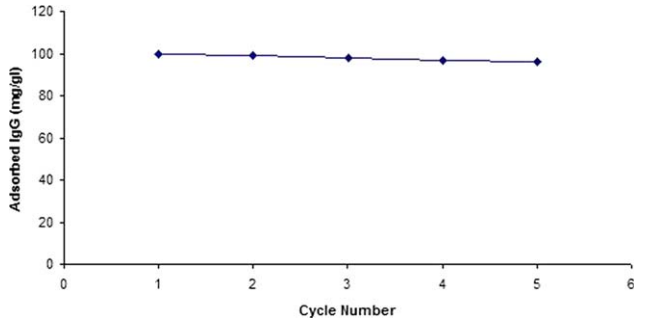

Figure 9. Repeated use of the spherical HA microcomposites (temperature = 25°C). [Color figure can be viewed in the online issue, which is available at wileyonlinelibrary.com.]

spontaneous behavior of the adsorption process, as discussed by Mohsen Nia et al.[40]

Effect of the Ionic Strength. Figure 8 presents the effect of the ionic strength on the h-IgG adsorption capacity. The adsorption capacity decreased with increasing ionic strength. The h-IgG adsorption on the spherical HA microcomposites decreased by about 80%, whereas the concentration of NaCl changed from 0 to 0.5*M*.[7] It was obvious that there was no significant change when a small amount of sodium chloride was used.[6,41,42] The decrease in the adsorption capacity as the ionic strength increased may have been due either to decreasing ionic interactions between the porous and spherical HA microcomposites and h-IgG molecules or to hydrophobic interactions between the h-IgG molecules themselves, which in turn, became stronger and caused the stacking of the h-IgG molecules. The presence of Na^+ and Cl^- ions in the medium may have caused a change in the adsorption of amino acids onto the porous and spherical HA microcomposites [poly(EGDMA) had a negligible adsorption capacity toward IgG].

Desorption and Repeated Use

The desorption of the adsorbed protein had to be done in the shortest time, and the highest amount of adsorbed protein had to be desorbed. Thus, the regeneration efficiency of the porous and spherical HA microcomposites after each cycle was very important. In this study, 97% of the adsorbed h-IgG molecules was desorbed easily from the porous and spherical HA microcomposites when sodium chloride was used as the desorption agent. The desorption studies were performed in a batch system. We concluded that NaCl was a suitable desorption agent for the desorption of h-IgG from the porous and spherical HA microcomposites (Figure 9).[43] To show the reusability of the porous and spherical HA microcomposites, the adsorption–desorption cycle was repeated five times with the same modified porous and spherical HA microcomposites from the aqueous h-IgG solution (Figure 9). There was no significant loss in the adsorption capacity of the beads after five cycles.

Comparison with Related Literature

A comparison of the IgG adsorption capacities for various composite materials is given in Table I. The adsorption capacity of the EGDMA/HA composite was higher than that of most of the microcomposites listed in Table I. The structure, functional

Table I. Comparison of the Adsorption Capacities for IgG of Various Composites

Composite	Amount of adsorption	Reference
Bent-His	15.6 mg/g	44
Ben-acrylamide-His	100 mg/g	45
Sintered HA	4 mg/m^2	46
Agarose- chitosan composite	71.4 mg/g	47
PHEMA/PGMA-IDA-Cu^{2+}	257 mg/g	48
Poly(ether sulfone)-chitosan	41.1 mg/g	49
Cellulose and acrylic		
Composite	15 mg/g	50
Chitosan-cellulose		
Composites	33.2 mg/g	51
m-Poly(GMA)-Con A	66.2 mg/g	2
EGDMA/HA composite	140.0 mg/g	This study

Bent: Bentonite; Ben-acrylamide-His: Bentonite-acrylamide-histidine; HA: Hydroxyapatite; PHEMA/PGMA-IDA: poly hydroxyethyl methacrylate/poly glycidyl methacrylate-iminodiasetic acid; *m*-Poly(GMA)-Con A: *m*-poly(glycidyl methacrylate)-Concanavalin A; EGDMA/HA: ethylene glicol dimethacrylate/hydroxyapatite.

groups, porosity, and surface area with the ligand caused the differences in the IgG adsorption capacity.

CONCLUSIONS

In this study, for the first time, porous and spherical HA microcomposites ranging from 50 to 100 μm in size were produced by suspension polymerization to improve the protein binding capacity of HA for h-IgG. The results show that the synthesized HA microcomposites had a porous structure, high surface area, high swelling behavior, and therefore higher h-IgG adsorption capacities than pure HA.

ACKNOWLEDGMENTS

This work was supported by the Research Fund of Cumhuriyet University (CUBAP, project number F-323). The author is also grateful to Recep Akkaya for valuable experimental studies.

REFERENCES

1. Duffy, S. A.; Moallering, B. J.; Prior, G. M.; Doyle, K. R.; Prior, C. P. *Pharm. Technol. Int.* **1989**, *1*(3), 46.
2. Akaya, B.; Candan, F.; Yavuz, H.; Denizli, A. *J. Appl. Polym. Sci.* **2012**, 125, 1867.
3. Kandori, K.; Miyagawa, K.; Ishikawa, T. *J Colloid Inter Sci.* **2004**, *273*, 406.
4. Denizli, A.; Alkan, M.; Garipcan, B.; Özkara, S.; Pişkin, E. *J. Chromatogr. B.* **2003**, *795*, 93.
5. Babac, C.; Yavuz, H.; Galaev, I. Y.; Pişkin, E.; Denizli, A. *React. Funct. Polym.* **2006**, *66*, 1263.
6. Ng, P.; He, J.; Gagnon, P. *J. Chromatogr. A* **2007**, *1142*, 13.
7. Gagnon, P. N. *Biotechnology* **2009**, *25*, 287.
8. Denizli, A. *Hacettepe J. Biol. Chem.* **2011**, *39*, 1.
9. Gagnon, P. An Enigma Unmasked: How Hydroxyapatite Works, and How to Make It Work For You; Validated Biosystems, Inc., **1998**.
10. Gorbunoff, M. *J. Anal. Biochem.* **1984**, *136*, 425.
11. Gorbunoff, M. *J. Anal. Biochem.* **1984**, *136*, 433.
12. Gagnon, P.; Cheung, C. W.; Yazaki, P. J. *J Sep. Sci.* **2009**, *32*, 3857.
13. Huang, P. Y.; Carbonell, R. G. *Biotechnol. Bioeng.* **1999**, *63*, 633.
14. Garipcan, B.; Denizli, A. *Macromol. Biosci.* **2002**, *2*, 135.
15. Roque, A. C. A.; Silva, C. S. O.; Taipa, M. Â. *J. Chromatogr. A* **2007**, *1160*, 44.
16. Yang, Z.; Yuan, H.; Tong, W.; Zou, P.; Chen, W.; Zhang, X. *Biomaterials* **1996**, *17*, 2131.
17. Jungbauer, A.; Hahn, R.; Deinhofer, K. *Biotechnol. Bioeng.* **2004**, *87*, 364.
18. Cummings, L. J.; Snyder, M. A.; Brisack, K. *Methods Enzymol.* **2009**, *463*, 387.
19. Mamone, G.; Picariello, G.; Ferranti, P.; Addeo, F. *Proteomics* **2010**, *10*, 380.
20. Williams, D. F. *Adv. Mater. Technol. Monitor* **1994**, *4*(2), 1.
21. Aoki, H. Science and Medical Applications of Hydroxyapatite, JAAS; Takayama Press System Center Co. Inc.: Tokyo, **1991**; pp 1–57, 85.
22. Veresov, A. G.; Putlyaev, V. I.; Tret'yakov, Y. D. *Ross Khim. Zh.* **2000**, *44*, 32.
23. Ulusoy, U.; Akaya, R. *J Hazard Mater.* **2009**, *163*, 98.
24. Xiao, X.; Liu, R.; Qiu, C.; Zhu, D.; Liu, F. *Mater. Sci. Eng. C* **2009**, *29*, 785.
25. Pradeesh, T. S.; Sunny, M. C.; Varma, H. K.; Ramesh, P. *Mater. Sci. Eng. C* **2005**, *28*, 383.
26. Fu, Q.; Rahaman, M. N.; Zhou, N.; Huang, W.; Wang, D.; Zhang, L.; Li, H. *J. Biomater. Appl.* **2008**, *23*, 37.
27. Zhao, Y.; Zhang, Y.; Ning, F.; Guo, D.; Xu, Z. *J. Biomed. Mater. Res. B* **2007**, *83*, 121.
28. Paul, W.; Sharma, S. T. *J. Mater. Sci. Mater. Med.* **1999**, *10*, 383.
29. Sarig, S.; Kahana, F. *Cryst. J Growth* **2002**, *55*, 237.
30. Sivakumar, M.; Manjubala, I.; Panduranga, K. R. *Carbohydr. Polym.* **2002**, *49*, 281.
31. Wang, Y.; Zhang, X.; Yan, J.; Xiao, Y.; Lang, M. *Appl. Surf. Sci.* **2011**, *257*, 6233.
32. Komlev, V. S.; Barinov, S. M.; Koplik, E. V. *Biomaterials* **2002**, *23*, 3449.
33. Akaya, B.; Uzun, L.; Candan, F.; Denizli, A. *Mater. Sci. Eng. C* **2007**, *27*, 180.
34. Ulusoy, U.; Akaya, R.; *J Hazard Mater.* **2009**, *163*, 98.
35. Sharpe, J. R.; Sammons, R. L.; Marquis, P. M. *Biomaterials* **1997**, *18*, 471.
36. Bundela, H.; Bajpai, A. K. *Express Polym. Lett.* **2008**, *2*, 201.

37. Özkara, S.; Akgöl, S.; Canak, Y.; Denizli, A. *Biotechnol. Prog.* **2004**, *20*, 1169.

38. Akgöl, S.; Ozkara, S.; Uzun, L.; Yılmaz, F.; Denizli, A. *J. Appl. Polym. Sci.* **2007**, *106*, 2405.

39. Luellau, E.; Stockar, U. V.; Vogt, S.; Freitag, R. *J. Chromatogr. A.* **1998**, *796*, 149.

40. Mohsen-Nia, M.; Massah Bidgoli, M.; Behrashi, M.; Mohsen Nia, A. *Protein J.* **2012**, *31*, 150.

41. Hansson, U. B.; Nilsson, E. *J. Immunol. Methods* **1973**, *2*, 221.

42. Josics, D. J.; Löster, K.; Kuhl, R.; Noll, F.; Reusch, J. *Biol. Chem. Hoppe-Seylars* **1991**, *372*, 149.

43. Kawasaki, T. *J. Chromatogr.* **1991**, *544*, 147.

44. Ozturk, N.; Tabak, A.; Akgol, S.; Denizli, A. *Colloids Surf. A* **2007**, *301*, 490.

45. Akaya, B. *Colloids Surf. B* **2012**, *92*, 151.

46. Svendsen, I. E.; Santos, O.; Sotres, J.; Wennerberg, A.; Breding, K.; Arnebrant, T.; Lindh, L. *Biofouling* **2012**, *28*, 87.

47. Sun, S.; Tang, Y.; Fu, Q.; Liu, X.; Guo, L.; Zhao, Y.; Chang, C. *Int. J. Biol. Macromol.* **2012**, *50*, 1002.

48. Bereli, N.; Şener, G.; Altıntaş, E. B.; Yavuz, H.; Denizli, A. *Mater. Sci. Eng. C.* **2010**, *30*, 323.

49. Klein, E.; Eichholz, E.; Theimer, F.; Yeager, D. *J. Membr. Sci.* **1994**, *95*, 199.

50. Hou, K. C.; Zaniewski, R.; Roy, S. *Biotechnol. Appl. Biochem.* **1991**, *13*, 257.

51. Yang, L.; Chen, P. *J. Membr. Sci.* **2002**, *205*, 141.